Article

Optical Spectroscopic Investigations of Model β-Sheet Hairpins in Aqueous Solution

Jovencio Hilario, Jan Kubelka, and Timothy A. Keiderling

J. Am. Chem. Soc., **2003**, 125 (25), 7562-7574• DOI: 10.1021/ja030039e • Publication Date (Web): 30 May 2003

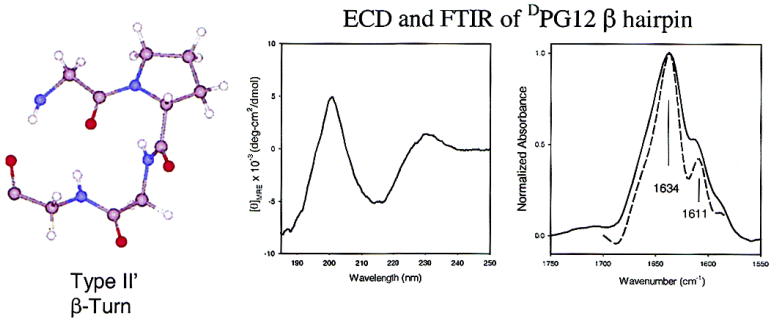

More About This Article

Additional resources and features associated with this article are available within the HTML version:

- Supporting Information
- Links to the 17 articles that cite this article, as of the time of this article download
- Access to high resolution figures
- Links to articles and content related to this article
- Copyright permission to reproduce figures and/or text from this article

View the Full Text HTML

J|A|C|S
ARTICLES
Published on Web 05/30/2003

Optical Spectroscopic Investigations of Model β-Sheet Hairpins in Aqueous Solution

Jovencio Hilario, Jan Kubelka, and Timothy A. Keiderling*

Contribution from the Department of Chemistry, University of Illinois at Chicago, 845 W. Taylor Street, Chicago, Illinois 60607-7061

Received January 21, 2003; E-mail: tak@uic.edu

Abstract: In this contribution we report optical spectroscopic data on a series of designed β hairpins previously shown by NMR to contain a substantial population of β-sheet structure. These models contain a designed hydrophobic cluster and a ^{D}Pro-Gly sequence to promote formation of a turn geometry. FTIR, electronic and vibrational CD (ECD and VCD) spectra for these small peptides are comparable to expected bandshapes for peptides of high β-sheet content. The ^{D}Pro-Gly sequence provides a better turn motif than Asn-Gly as measured by its β-sheet spectral characteristics. IR and VCD spectra are in qualitative agreement with theoretical simulations based on transfer of parameters from ab initio quantum mechanical force field and intensity computations for the turn and strands. These calculations provide assignments for some distinguishing modes in both IR and VCD spectra. Increased sheet structure can be induced in these hairpins by use of mixed solvent conditions. Thermal denaturation studies reveal that these hairpins undergo very broad unfolding transitions. Guanidine hydrochloride unfolding transitions for the selected hairpin models are similarly broad. However, the "end-states" of temperature and chaotropic denaturation are spectroscopically differentiable.

Introduction

Despite the great diversity in protein structure, most proteins are primarily composed of regular secondary structural elements. Proteins can be classified on the basis of their arrangement of relatively few secondary structure types. Of these, α helices and β sheets are most commonly observed.[1] Efforts aimed at shedding light on the details of the protein folding process have sought to use peptides as model systems for secondary structures found in proteins. This affords the examination of intrinsic factors controlling secondary structure formation and stability without the influence of tertiary structure effects. While most initial studies addressed α-helix formation,[2−4] β-sheet structure, formation, and stability are equally as important for answering questions about general processes of protein folding.[5,6] Heightened interest in understanding the factors affecting β-sheet formation is prompted by the fact that many degenerative diseases have their pathology rooted in protein or peptide aggregation, which often involves sheet formation.[7−10] Until recently, studies of β-sheet systems have lagged behind those of α helices, due to the difficulty in generating nonaggregating, water-soluble β-sheet models. However, now a wide variety of β-sheet models having some stability in aqueous solution have been synthesized to form two-, three-, and four-stranded sheet forms, as well as higher-order structures (through dimerization).[11−15]

Early studies on the simplest form of β-sheet structure, β hairpins, used sequences derived from or identical to those found in protein structures. These studies showed that while β hairpins or model sheets could form monomerically in an aqueous environment, the preparation of isolated sequences extracted from folded proteins does not often result in useful β-hairpin structures.[11] Tertiary contacts and, in particular, specific hydrophobic interactions are often important for stability and can be added to hairpins by incorporation of appropriate residues.[16,17]

Selected short peptides containing secondary structure elements (helices, sheets, turns) have been shown to unfold from the ends with the equilibrium structure best represented as an ensemble of microstates.[18−21] A complex balance of different factors are involved in forming the associated strands of a β sheet (i.e. hydrogen bonding, hydrophobic, side chain−side

(1) Creighton, T. E. *Proteins: Structures and Molecular Properties*, 2nd ed.; W. H. Freeman and Co.: New York, 1993.
(2) Zimm, B. H.; Bragg, J. K. *J. Chem. Phys.* **1959**, *31*, 526.
(3) Nevskaya, N. A.; Chirgadze, Y. N. *Biopolymers* **1976**, *15*, 637.
(4) Scholtz, J. M.; Baldwin, R. L. *Annu. Rev. Biophys. Biomol. Struct.* **1992**, *21*, 95.
(5) Salemme, F. R. *Prog. Biophys. Mol. Biol.* **1983**, *42*, 95.
(6) Nesloney, C. L.; Kelly, J. W. *Bioorg. Med. Chem.* **1996**, *4*, 739.
(7) Harper, J. D.; Lansbury, P. T. *Annu. Rev. Biochem.* **1997**, *66*, 385.
(8) Prusiner, S. B. *Proc. Natl. Acad. Sci. USA* **1998**, *95*, 13363.
(9) Fink, A. J. *Folding Des.* **1998**, *3*, R9.
(10) Serpell, L. C. *Biochim. Biophys. Acta* **2000**, *1502*, 16.
(11) Gellman, S. H. *Curr. Opin. Struct. Biol.* **1992**, *2*, 717.
(12) de Alba, E.; Santoro, J.; Rico, M.; Jimenez, M. A. *Protein Sci.* **1999**, *8*, 854.
(13) Schenck, H. L.; Gellman, S. H. *J. Am. Chem. Soc.* **1998**, *120*, 4869.
(14) Kortemme, T.; Ramirez-Alvarado, M.; Serrano, L. *Science* **1998**, *281*, 253.
(15) Das, C.; Nayak, V.; Raghothama, S.; Balaram, P. *J. Pept. Res.* **2000**, *56*, 307.
(16) Cochran, A. G.; Skelton, N. J.; Starovasnik, M. A. *Proc. Natl. Acad. Sci. U.S.A.* **2001**, *98*, 5578.
(17) Tatko, C. D.; Waters, M. L. *J. Am. Chem. Soc.* **2002**, *124*, 9372.
(18) Silva, R. A. G. D.; Kubelka, J.; Decatur, S. M.; Bour, P.; Keiderling, T. A. *Proc. Natl. Acad. Sci. U.S.A.* **2000**, *97*, 8318.
(19) Rohl, C. A.; Baldwin, R. L. *Biochemistry* **1994**, *33*, 7760.
(20) Yoder, G.; Pancoska, P.; Keiderling, T. A. *Biochemistry* **1997**, *36*, 15123.
(21) Munoz, V.; Thompson, P. A.; Hofrichter, J.; Eaton, W. A. *Nature* **1997**, *390*, 196.

10.1021/ja030039e CCC: $25.00

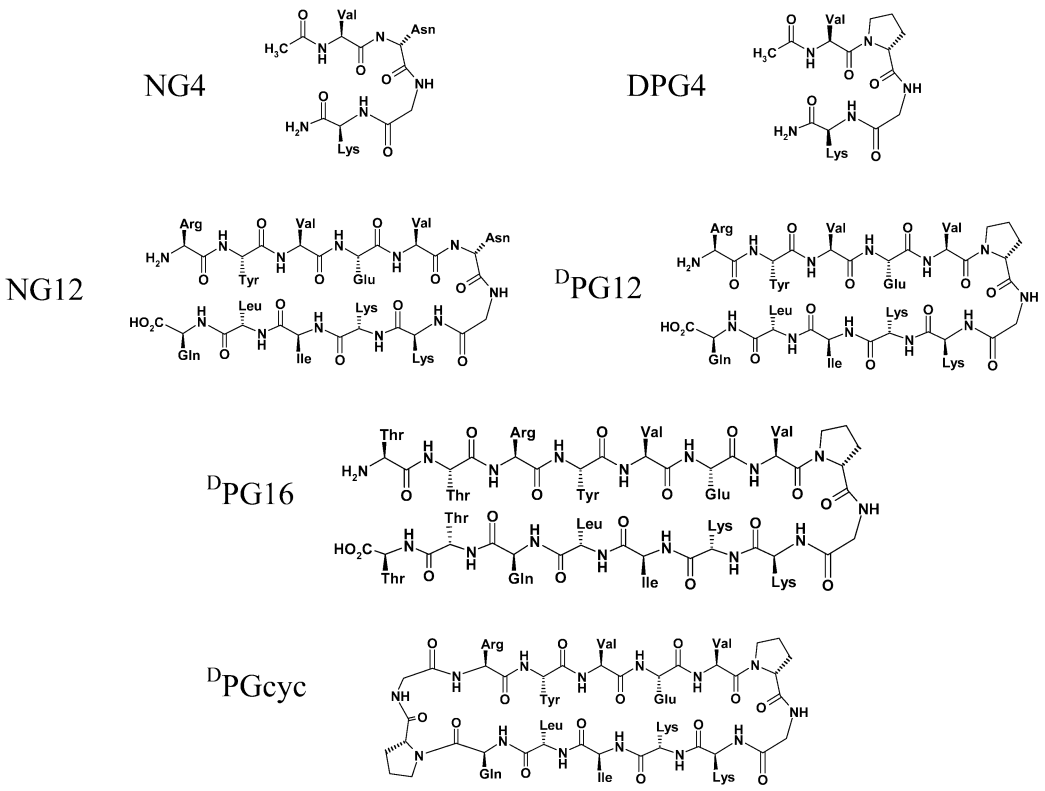

Figure 1. Schematic structures of selected β turns and β hairpins used in this study. The idealized turn or hairpin forms are represented.

chain interactions, and turn geometry).[22] An argument against the stability of small peptide motifs is that, at least for small peptide β sheets (two- and three-stranded with less than ~50 residues), the domain is not stable at physiological conditions.[23] Consistent with this, two model three-strand β-sheet peptides were shown to unfold in a noncooperative thermal transition.[24] Yet for some β-sheet proteins and mini-protein motifs, evidence for cooperative behavior has been found both in equilibrium and kinetic unfolding/refolding experiments.[25−29]

From a statistical analysis of selected protein structures it was discovered that while type I and II β-turns, which differ only in their central ψ_{i+1}, ϕ_{i+2} torsion angles, are generally favored in loop structures, the mirror-image β-turns, types I′ and II′, were most commonly found in tight, two-residue turns.[30] These latter turns also were observed to produce a twist that is favorable to the alignment of attached β strands.[31] Recently, Gellman and co-workers[32−35] and Balaram and co-workers[36,37] have synthesized a variety of β-sheet hairpins containing type II′ (or I′) turns stabilized by a D-amino acid (^{D}Pro) and Gly in the $i + 1$ and $i + 2$ positions of the loop. NMR studies of these hairpins indicated that they contain a high population of sheetlike contacts between strands. More recent NMR results suggested that, while β-hairpin stability initially increases with increasing strand length, an intrinsic limit is found if strands are further lengthened with just threonine.[35]

Optical spectroscopic techniques typically result in averaged conformational information as compared to more site-specific methods (NMR, X-ray) yet are often preferred due to ease of sample preparation, the need for small quantities and moderate concentrations, and their intrinsically fast time scale for monitoring conformational change and fluctuation. When combined with various multivariate and regression analysis methods, optical spectral data can be used to estimate the percent of secondary structure and their changes.[38−43] In this study, we characterize several β-hairpin models taken directly from designs of Gellman[32,33] using FTIR absorbance, electronic circular dichroism (ECD, in the UV), and vibrational circular dichroism (VCD, in the IR) spectroscopies. We examine unblocked peptides (Figure 1) with 12 residues (the two residues in the turn are underlined in the sequence), Arg-Tyr-Val-Glu-Val-Asn-Gly-Lys-Lys-Ile-

(22) Griffiths-Jones, S. R.; Sharman, G. J.; Maynard, A. J.; Searle, M. S. *J. Mol. Biol.* **1998**, *284*, 1597.
(23) Privalov, P. L. *Annu. Rev. Biophys. Biophys. Chem.* **1989**, *18*, 47.
(24) Kuznetsov, S. V.; Hilario, J.; Keiderling, T. A.; Ansari, A. *Biochemistry* **2003**, *42*, 4321.
(25) Schoenbrunner, N.; Pappenberger, G.; Scharf, M.; Engels, J.; Kiefhaber, T. *J. Mol. Biol.* **1997**, *268*, 526.
(26) Clark, P. L.; Weston, B. F.; Gierasch, L. M. *Folding Des.* **1998**, *3*, 401.
(27) Koepf, E. K.; Petrassi, H. M.; Sudol, M.; Kelly, J. W. *Protein Sci.* **1999**, *8*, 841.
(28) Neidigh, J. W.; Fesinmeyer, R. M.; Andersen, N. H. *Nat. Struct. Biol.* **2002**, *9*, 425.
(29) Honda, S.; Kobayashi, N.; Munekata, E. *J. Mol. Biol.* **2000**, *295*, 269.
(30) Sibanda, B. L.; Thornton, J. M. *Nature* **1985**, *316*, 170.
(31) Chothia, C. J. *J. Mol. Biol.* **1973**, *75*, 295.
(32) Syud, F. A.; Espinosa, J. F.; Gellman, S. H. *J. Am. Chem. Soc.* **1999**, *121*, 11577.
(33) Haque, T. S.; Gellman, S. H. *J. Am. Chem. Soc.* **1997**, *119*, 2303.
(34) Stanger, H. E.; Gellman, S. H. *J. Am. Chem. Soc.* **1998**, *120*, 4236.
(35) Stanger, H. E.; Syud, F. A.; Espinosa, J. F.; Giriat, I.; Muir, T.; Gellman, S. H. *Proc. Natl. Acad. Sci. U.S.A.* **2001**, *98*, 12015.
(36) Ragothama, S. R.; Awasthi, S. K.; Balaram, P. *J. Chem. Soc., Perkin Trans.* **1998**, *2*, 137.
(37) Zhao, C.; Polavarapu, P. L.; Das, C.; Balaram, P. *J. Am. Chem. Soc.* **2000**, *122*, 8228.
(38) Venyaminov, S. Y.; Yang, J. T. In *Circular Dichroism and the Conformational Analysis of Biomolecules*; Fasman, G. D., Ed.; Plenum Press: New York, 1996; p 69.
(39) Hennessey, J. P.; Johnson, W. C. *Biochemistry* **1981**, *20*, 1085.
(40) Johnson, W. C. *Annu. Rev. Biophys. Biophys. Chem.* **1988**, *17*, 145.
(41) Pancoska, P.; Bitto, E.; Janota, V.; Urbanova, M.; Gupta, V. P.; Keiderling, T. A. *Protein Sci.* **1995**, *4*, 1384.
(42) Baumruk, V.; Pancoska, P.; Keiderling, T. A. *J. Mol. Biol.* **1996**, *259*, 774.
(43) Keiderling, T. A.; Kubelka, J.; Hilario, J. In *Vibratonal spectrroscopy of polymers and biological systems*; Braiman, M., Gregoriou, V., Eds.; Marcel Dekker: Amsterdam, New York, in press.

Leu-Gln (NG12) and Arg-Tyr-Val-Glu-Val-^{D}Pro-Gly-Lys-Lys-Ile-Leu-Gln (^{D}PG12), to compare turn propensity effects, and the sixteen residue peptide Thr-Thr-Arg-Tyr-Val-Glu-Val-^{D}Pro-Gly-Lys-Lys-Ile-Leu-Gln-Thr-Thr (^{D}PG16) to model length effects. These are compared to results from a cyclic peptide, Arg-Tyr-Val-Glu-Val-^{D}Pro-Gly-Lys-Lys-Ile-Leu-Gln-^{D}Pro-Gly (^{D}PGcyc), with the same core sequence as above, which previously has been used as a reference for the fully formed antiparallel β-hairpin state.[32] Finally, two four-residue blocked peptides, Ac-Val-Asn-Gly-Lys-NH_2 (NG4) and Ac-Val-^{D}Pro-Gly-Lys-NH_2 (^{D}PG4), are used as reference models for the isolated turn contribution. We show that model hairpins containing the ^{D}Pro-Gly turn sequence develop optical spectral characteristics comparable to those of β-sheet proteins. We also present results of thermal denaturation studies for selected β-hairpin peptides as monitored by ECD and FTIR. Temperature-dependent spectra reveal a reversible loss of secondary structure for these hairpin models which display broad unfolding transitions. Additional unfolding experiments were performed with guanidine hydrochloride (GdnHCl), yielding results that are spectrally distinct from the thermal denaturation ECD spectra. Their different spectral responses demonstrate that the final "end states" of the chaotropic (chemical) and thermal denaturation experiments are indeed distinguishable.

Experimental Section

Samples. All linear peptide samples were synthesized using standard solid-phase Fmoc chemistry. The cyclic peptide was synthesized using an orthogonally protected glutamic acid derivative and standard solid-phase synthesis. Samples of ^{D}PG12 and ^{D}PGcyc (Figure 1) generously provided by Professor S. H. Gellman, University of Wisconsin, and used in preliminary studies were prepared in his laboratory by Faisal Syud as previously reported.[32,34,35] The remaining peptides, ^{D}PG16, NG4, and ^{D}PG4, and further quantities of the initial samples were subsequently synthesized locally at the UIC Protein Research Facility again using standard peptide synthesis protocols and were HPLC-purified and analyzed by electrospray mass spectrometry to verify molecular weight. Samples from both sources exhibited the same IR and ECD spectra in 10 mM acetate buffered H_2O and D_2O solutions.

Measurements. ECD measurements were performed on a Jasco J-810 (or J-600) spectropolarimeter (Easton, MD) equipped with a thermostated cell holder. Spectra of peptides at a concentration of ~0.15 mg/mL (80−100 μM) in 10 mM acetate/H_2O buffer (pH 3.8) were recorded over the 185−250 nm wavelength region and in the temperature range of 5−90 °C (every 5°) with a 2 s response time and a scanning speed of 50 nm/min. For titration experiments in TFE, stock solutions of peptides were prepared and diluted to a final concentration of ~0.15 mg/mL in the appropriate buffer/TFE concentration. To obtain spectra over a range of GdnHCl concentrations for selected hairpins, samples prepared at 1.5 mg/mL were used with a 0.1-mm path length cylindrical quartz cell.

Generally, for each condition, 4−8 scans were averaged for spectra collected at scan speeds of 20 or 50 nm/min with 0.2-nm step size, 1.0-nm bandwidth, and a 2.0-s response time. All sample spectra were subsequently baseline-subtracted using a similarly obtained spectrum of buffer. Where applicable, ECD spectra were converted to units of molar ellipticity using concentrations determined from the absorbance measured at 280 nm, using an extinction coefficient of 1280 M^{-1} cm^{-1} for the single tyrosine residue in each peptide.[44] No difference was observed in the 280 nm absorbances determined in native or denaturing (6 M GdnHCl) conditions, indicating that Tyr was solvent-accessible in both. Concentrations for the turn models without Tyr were determined by mass.

FTIR measurements were recorded on either a Bio-Rad FTS-60 or FTS-60A spectrometer. To remove trifluroacetic acid (TFA), whose absorption can interfere with the amide I′ band, peptide samples were repeatedly treated with 10 mM DCl in D_2O (pH 2.3 uncorrected) and lyophilized. The process was repeated until the absorbance of TFA was completely removed or significantly diminished with respect to the amide I′ peak of the peptide. This step also effected H/D exchange of the samples. Peptides for IR thermal denaturation experiments were prepared at 10 mg/mL (~5−7 mM) in 10 mM acetate/D_2O (pH 3.8 uncorrected) buffer and placed in a homemade IR cell containing CaF_2 windows with a 50-μm Teflon spacer fastened with a brass mounting ring. For thermal denaturation measurements from ~5−91 °C at ca. 4 °C intervals, the homemade cell is placed inside a brass water-jacketed holder which is attached to a Neslab circulating water bath. The temperature of the cell is determined by a probe whose output is used to control the bath temperature. Unless noted, reported FTIR frequencies are obtained from second derivative analysis of the absorbance spectrum.

Vibrational circular dichroism (VCD) spectra were collected on the UIC dispersive spectrometer which has been described in detail previously.[43,45] Samples were prepared at 20−40 mg/mL in 10 mM acetate/D_2O buffer, and the same TFA removal/H−D exchange methods as described for FTIR were used. Typically 8−12 scans were averaged and baseline-corrected by subtracting the corresponding average of buffer scans. No change in FTIR spectral band shape was seen in test spectra for ^{D}PG12 and ^{D}PGcyc spanning the concentration ranges used in the ECD and VCD measurements (1−40 mg/mL). This concentration independence has been shown in previous work by Gellman and coworkers.[33,35]

Temperature-dependent FTIR and ECD spectra were first processed with a singular value decomposition (SVD)[46] filter implemented in Matlab (The MathWorks, Inc., Natick, MA). This transforms the raw data matrix, **D**, according to $\mathbf{D} = \mathbf{USV}^{T}$, where **U** is the matrix of basis set spectra describing the data, **V** is the matrix of amplitude values as a function of condition, and **S** is the diagonal matrix containing singular values describing the contribution of basis spectra to the data set. For FTIR spectra it was found that greater than 99% of the spectral response could be reconstructed from just the first two-component spectra and temperature-varying amplitudes. However, for ECD spectra, four-component spectra were required to obtain 95% of the spectral variation. For both FTIR and ECD, the first component spectrum represents the average intensity of the data, while the second component reveals the major spectral variation as a function of temperature.

Calculational Methods. The structure of ^{D}PGcyc derived from analysis of its NMR spectra[32] was used to create segments of a hairpin structure appropriate for ab initio quantum mechanical calculation of spectral parameters. The two turn geometries (one roughly type I′ and the other type II′) in this cyclic peptide were both simulated using a sequence, Ac-AA^{D}PGAA-CH_3 (A = Ala, G = Gly, ^{D}P = D-Pro), constrained to the NMR determined ϕ, ψ angles for that turn.[47] All other geometrical parameters were optimized using density functional theory (DFT) computations at the BPW91/6-31G* level as implemented in the Gaussian 98 program package.[48] The force field (FF) and atomic polar and axial tensors (APT, AAT) were then computed at the same level of theory for the optimized geometry. The antiparallel strand geometry for the model hairpin was also obtained from the ^{d}PGcyc structure and modeled as two Ac-AA-$NHCH_3$ strands aligned in the antiparallel direction and hydrogens bonded to each other.

(44) Gill, S. C.; von Hippel, P. H. *Anal. Biochem.* **1989**, *182*, 319.
(45) Keiderling, T. A. In *Practical Fourier Transform Infrared Spectroscopy*; Krishnan, K., Ferraro, J. R., Eds.; Academic Press: San Diego, 1990; p 203.
(46) Hendler, R. W.; Shrager, R. I. *J. Biochem. Biophys. Methods* **1994**, *28*, 1.
(47) Gellman, S. H. Personal communication.

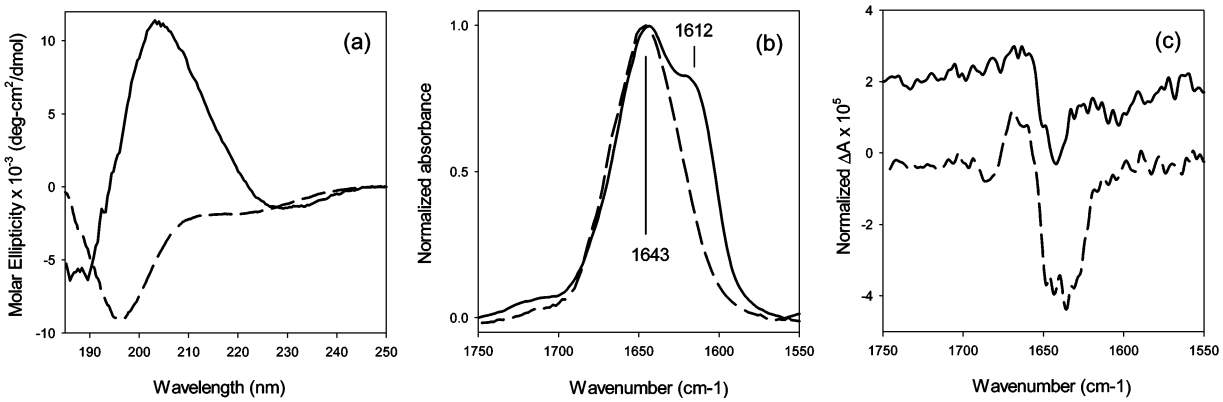

Figure 2. (a) ECD, (b) FTIR absorbance, and (c) VCD spectra for the two four-residue β turns, NG4 (dashed) and ^{D}PG4 (solid). All spectra were recorded at 5 °C. The same sample of each was measured for FTIR and VCD. ECD spectra are in 10 mM acetate/H_2O at ~0.15 mg/mL peptide in 1 mm path length. IR and VCD are in 10 mM acetate/D_2O at 20−40 mg/mL peptide in 50 μm path length. Molar ellipticity is expressed per residue.

Spectra of a full β hairpin were simulated by transferring the ab initio computed FF, APT, and AAT tensor elements from these segments onto the appropriate atoms of the larger structure, simulated as Ac-AAAAA^{D}PGAAAAA-CH_3 for direct comparison to ^{D}PG12. These transfers used our established property transfer method[49] but with its code modified to choose the best fit to the local (large) peptide geometry from two basis (small) peptide computations.[50] Spectra were simulated by positioning and weighting Lorentzian band shapes of 15 cm^{-1} full width at half-maximum at the computed frequency of each transition and scaling their area to the computed dipole or rotational strengths to obtain the IR absorption or VCD spectrum, respectively. To obtain a comparison for proteinogenic residues in the turn, such as NG, independent calculations were carried out for the Ac-AAGA-$NHCH_3$ sequence and compared to results for Ac-A^{D}PGA-$NHCH_3$, both constrained to the same type I′ turn geometry.[50]

Results

Spectra. To examine the effect that the turn geometry has on the optical spectroscopic properties of these selected β hairpins, namely the ECD $n-\pi^*$, $\pi-\pi^*$, and the IR and VCD amide I′ (C═O stretching, N-deuterated) transitions, we first sought to investigate the optical spectra for just the turn portion of the β-hairpin models using the four-residue N and C terminally blocked peptides NG4 and ^{D}PG4 whose ECD, IR, and VCD spectra at 5 °C are presented in Figure 2a−c.

The ECD spectra (Figure 2a) for the NG4 turn model in 10 mM acetate/H_2O buffer displays a characterstic random coil type spectrum with an intense minimum at 196 nm. However, the spectrum obtained for the ^{D}PG4 turn model is similar to that assigned to type II turns, as found for cyclic hexamer peptides,[51] with a minimum below 190 nm and an exceptionally intense, for such a short peptide, maximum ellipticity at 203 nm.

IR spectra of NG4 and ^{D}PG4 in 10 mM acetate/D_2O buffer (Figure 2b), have surprisingly similar peak absorbance frequencies for the main amide I′ band. However, second derivative IR spectra identify five-component bands (there are five amides in these turn models, including blocking groups) for the ^{D}PG4 model, while only four components are found in the NG4 model. Two differences exist in the second derivative amide I′ spectra for these two turn models: a component at 1667 cm^{-1} in NG4 shifts to 1658 cm^{-1} in ^{D}PG4, and ^{D}PG4 possesses a lower-frequency band at 1612 cm^{-1}. The latter is due to the specific Val-^{D}Pro tertiary amide linkage in contrast to the Val-Asn amide bond vibration which is overlapped with the main amide I′ band (Table 1).

VCD spectra (Figure 2c) for both peptides in 10 mM acetate/D_2O (same samples as for IR) are dominated by negative couplets with a band shapes qualitatively mimicking those determined empirically for random coil conformations.[52,53] In the ^{D}PG4 model the effect of the lower-frequency tertiary amide can be seen as a negative shoulder while this component is missing in the NG4 VCD. However, the normalized intensity of the main negative VCD band of NG4 is effectively double that of ^{D}PG4, suggesting a difference in the source of this band shape for these two peptides.

The two hairpin models, NG12 and ^{D}PG12, differ only in the $i + 1$ position of the turn. Comparison of their ECD and FTIR spectra measured at 5 °C (Figure 3), indicates that the sequence containing the ^{D}Pro-Gly turn (^{D}PG12) forms a more developed hairpin (β-structure) than does the sequence containing an Asn-Gly turn (NG12). The ECD band shape for the ^{D}PG12 hairpin contains aspects suggestive of band shapes found in representative β-sheet spectra,[38,54] i.e. a minimum at 215 nm,

(48) Frisch, M. J.; Trucks, G. W.; Schlegel, H. B.; Scuseria, G. E.; Robb, M. A.; Cheeseman, J. R.; Zakrzewski, V. G.; Montgomery, J. J. A.; Stratmann, R. E.; Burant, J. C.; Dapprich, S.; Millam, J. M.; Daniels, A. D.; Kudin, K. N.; Strain, M. C.; Farkas, O.; Tomasi, J.; Barone, V.; Cossi, M.; Cammi, R.; Mennucci, B.; Pomelli, C.; Adamo, C.; Clifford, S.; Ochterski, J.; Petersson, G. A.; Ayala, P. Y.; Cui, Q.; Morokuma, K.; Malick, D. K.; Rabuck, A. D.; Raghavachari, K.; Foresman, J. B.; Cioslowski, J.; Ortiz, J. V.; Stefanov, B. B.; Liu, G.; Liashenko, A.; Piskorz, P.; Komaromi, I.; Gomperts, R.; Martin, R. L.; Fox, D. J.; Keith, T.; Al-Laham, M. A.; Peng, C. Y.; Nanayakkara, A.; Gonzalez, C.; Challacombe, M.; Gill, P. M. W.; Johnson, B.; Chen, W.; Wong, M. W.; Andres, J. L.; Gonzalez, C.; Head-Gordon, M.; Replogle, E. S.; Pople, J. A. *Gaussian 98*; Revision A.6 ed.; Frisch, M. J.; Trucks, G. W.; Schlegel, H. B.; Scuseria, G. E.; Robb, M. A.; Cheeseman, J. R.; Zakrzewski, V. G.; Montgomery, J. J. A.; Stratmann, R. E.; Burant, J. C.; Dapprich, S.; Millam, J. M.; Daniels, A. D.; Kudin, K. N.; Strain, M. C.; Farkas, O.; Tomasi, J.; Barone, V.; Cossi, M.; Cammi, R.; Mennucci, B.; Pomelli, C.; Adamo, C.; Clifford, S.; Ochterski, J.; Petersson, G. A.; Ayala, P. Y.; Cui, Q.; Morokuma, K.; Malick, D. K.; Rabuck, A. D.; Raghavachari, K.; Foresman, J. B.; Cioslowski, J.; Ortiz, J. V.; Stefanov, B. B.; Liu, G.; Liashenko, A.; Piskorz, P.; Komaromi, I.; Gomperts, R.; Martin, R. L.; Fox, D. J.; Keith, T.; Al-Laham, M. A.; Peng, C. Y.; Nanayakkara, A.; Gonzalez, C.; Challacombe, M.; Gill, P. M. W.; Johnson, B.; Chen, W.; Wong, M. W.; Andres, J. L.; Gonzalez, C.; Head-Gordon, M.; Replogle, E. S.; Pople, J. A. *Gaussian 98*; Gaussian, Inc.: Pittsburgh, PA, 1998.
(49) Bour, P.; Sopkova, J.; Bednarova, L.; Malon, P.; Keiderling, T. A. *J. Comput. Chem.* **1997**, *18*, 646.
(50) Kubelka, J. Ph.D. Thesis, Department of Chemistry, University of Illinois at Chicago, Chicago, 2002.
(51) Rose, G. D.; Gierasch, L. M.; Smith, J. A. *Adv. Protein Chem.* **1985**, *37*, 1.
(52) Dukor, R. K.; Keiderling, T. A. *Biopolymers* **1991**, *31*, 1747.
(53) Keiderling, T. A.; Silva, R. A. G. D.; Yoder, G.; Dukor, R. K. *Bioorg. Med. Chem.* **1999**, *7*, 133.
(54) Greenfield, N.; Fasman, G. D. *Biochemistry* **1969**, *8*, 4108.

Table 1. Frequency Components of the Amide I′ Band for Selected β-Turn and β-Hairpin Models[a]

	frequency (cm^{-1})					
molecule	turn	turn	unordered		sheet	3° amide
NG4	1680	1667	1648	1643		
^{D}PG4	1680	1658	1650	1643		1612
NG12[b]	1690	1658		1640		
		(1658, *0.20*)		(1640, *0.71*)		
^{D}PG12		1668, 1659	1649		1634	1611
		(1658, *0.28*)			(1636, *0.51*)	(1609, *0.21*)
^{D}PG16	1678	1663	1649		1634	1609
			(1655, 0.*50*)		(1636, *0.40*)	(1609, *0.10*)
^{D}PGcyc	1681	1665	1650		1635	1613
	(1680, *0.01*)	(1663, *0.07*)	(1649, *0.27*)		(1635, *0.33*)	(1613, *0.32*)

[a] Frequency assignments determined from second derivative analysis. Values in parentheses refer to peak center position (cm^{-1}) and percent area (italics) based on curve-fitting of the deconvolved spectrum. [b] The weak, deconvolved band at 1612 cm^{-1} in NG12 (not listed) cannot be due to tertiary amide, and probably results from a side chain mode. However, it and the weak 1690 cm^{-1} band could indicate a small degree of aggregation in this unfolded sample.

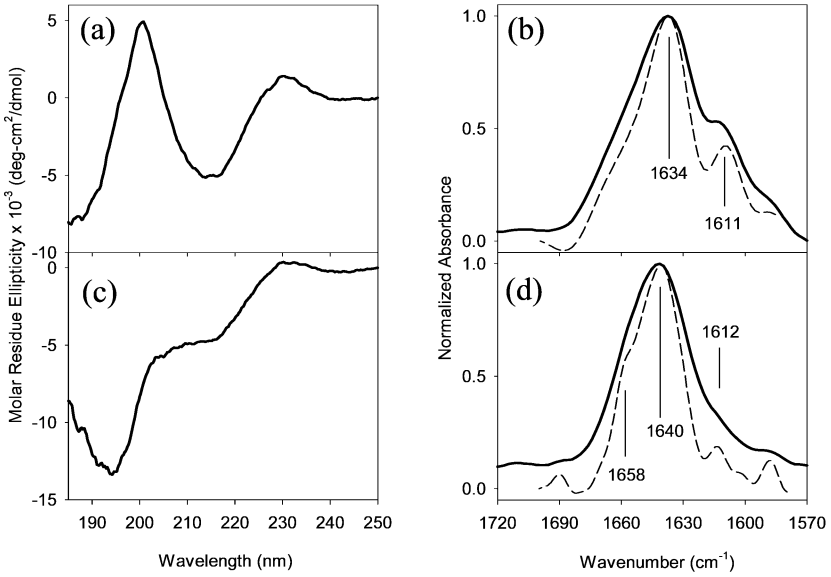

Figure 3. ECD (a,c) and FTIR (b, d) spectra for β-hairpin models, ^{D}PG12 (a,b) and NG12 (c,d). ECD and FTIR spectra reveals better β-hairpin formation in the ^{D}PG12 model, with NG12 displaying a greater spectral contribution from the random coil component. Dashed line FTIR spectra are Fourier deconvolved spectra. Spectra were recorded at 5 °C with same sample conditions as in Figure 2.

a zero-crossing at 205 nm, and a positive at ~200 nm. The positive ECD is reduced in intensity due to overlap with a negative band at ~185 nm, echoing features in the ^{D}PG4 turn ECD (Figure 2). The FTIR spectrum of the ^{D}PG12 hairpin yields an amide I′ absorbance maximum at 1634 cm^{-1} consistent with formation of a cross-strand β-sheet (hydrogen bond) interaction. In addition, a lower-frequency band appears at 1611 cm^{-1}, due to the tertiary amide (Val-^{D}Pro), here additionally hydrogen bonded in a stable β-turn conformation.[55] The spectral data of the Asn-Gly turn-based hairpin (NG12) reveals a large random coil-like contribution as evidenced by the large negative ECD band at 195 nm, correlated with a shift of the amide I′ band to higher frequency (1640 cm^{-1}). The various underlying FTIR components are enhanced by Fourier self-deconvolution (dashed lines).

The ECD, FTIR, and VCD spectra as a function of length and stability are compared in Figure 4a−c for the four ^{D}Pro-Gly turn-containing peptides, ^{D}PG4, ^{D}PG12, ^{D}PG16, and ^{D}PGcyc at 5 °C. The ECD band shapes for these related structures show both simple and complex features. An increasing ECD spectral intensity is seen at ~215 nm, consistent with forming more β-sheet structure upon increased strand length or conformational rigidity, with the ECD spectrum for the ^{D}PGcyc model being the most sheetlike (judged by the peak-to-peak intensity of the 215 and 200 nm bands).[38] While the ECD spectrum of ^{D}PG12 has considerable sheet character, the ^{D}PG16 spectrum shows a lower ECD intensity at 216 nm and an increased random coil contribution evidenced at 195 nm. The balance of coil and sheet contributions can lead to a significant distortion in ECD band shape[56] so that quantitative evaluation of β-sheet content should not be made from the 216 nm intensity alone.

FTIR spectra were analyzed by second derivative, deconvolution, and curve-fitting analyses and the results are summarized in Table 1. All ^{D}Pro-Gly containing models display an amide I′ maximum at ~1635 cm^{-1} and a low-frequency component at 1609−1613 cm^{-1}, the latter attributable to the Val-^{D}Pro tertiary amide in the turn (see comparison, Figure 2).[55] Resolution enhancement (dashed line spectra, Figure 4) shows a variable contribution from higher-frequency components as well. Approximately 30% of the amide I′ area for ^{D}PG12 and ^{D}PGcyc

(55) Xie, P.; Diem, M. *J. Am. Chem. Soc.* **1995**, *117*, 384.

(56) Sreerama, N.; Woody, R. W. *Protein Sci.* **2003**, *12*, 384.

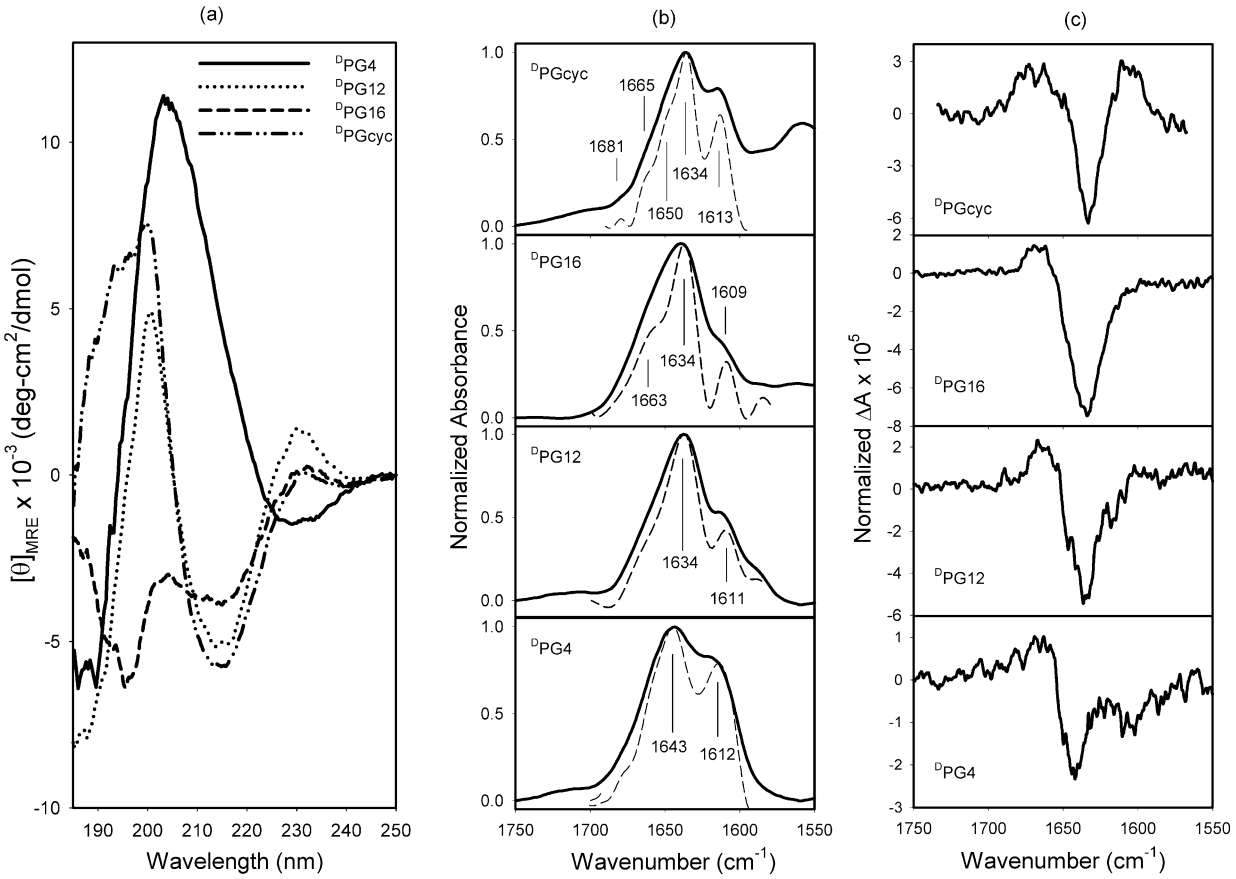

Figure 4. ECD (a), FTIR (b), VCD (c) spectra for DPro-Gly containing β-turn and β-hairpin models. All spectra were measured at 5 °C. Sample conditions are the same as in Figure 3.

arise from components fit to the deconvolved bands at 1658 and 1649 cm^{-1} respectively (Table 1), with DPG16 having ~50% contribution from a component at 1655 cm^{-1}. These contributions might reasonably be expected to arise from amides in random coil or turn conformations. By comparison DPG4, containing just the turn, lacks the ~1635 cm^{-1} β-sheet feature; with its main amide I′ appearing at 1646 cm^{-1}.

For the NG12 hairpin, 71% of the FTIR amide band integrated area comes from the component at 1640 cm^{-1}, which may arise in part from β-sheet hydrogen-bonded carbonyls, but has significant intensity due to the random coil components. This band could not be further deconvolved to separate random coil from β-sheet contributions. By contrast, for DPG12 and DPG16 we observe the main amide I′ intensity at a lower frequency, 1634 cm^{-1}, with respective areas of 51% and 40%, suggesting sheetlike character of the amides (H-bonded in β-conformation leading to interstrand coupling[57]) and again showing, as did the ECD, that DPG16 actually contains a smaller fractional β-sheet content than does the shorter DPG12. This is also consistent with the percent contribution from higher frequency modes. For DPG12, 28% of the amide I′ area stems from a component at 1658 cm^{-1} (random coil/turn), while for DPG16, 50% of the amide I′ area corresponds to a component at 1655 cm^{-1} (Table 1 and Figure 4). Surprisingly, the DPGcyc model (presumably the most stable β hairpin) only yields 33% of its amide I′ contributing at 1635 cm^{-1} but with a 32% contribution from the tertiary amides of both DPro-Gly turns. The implication of this to sheet formation and to the validity of using IR band intensities in a simple additive manner for such discrimination is addressed in the Discussion

The vibrational CD (VCD) spectra are all characteristic of structures with a local left-handed twist and could be viewed as being qualitatively consistent with either random coil or some (twisted, proteinogenic) β-sheet structures. The strong correlation of the negative VCD lobe with the intense IR amide I′ peak along with the character of the observed ECD spectra (with the exception of DPG4) suggests some contribution from β-sheet structure.[58] The negative VCD band correlated with the Val-DPro absorption (1612 cm^{-1}) seen for DPG4 is possibly detectable in the DPG12 result but is undetectable in DPG16. However, the same band in DPGcyc becomes a positive lobe (lying on the low-frequency side of the main negative band) which may result from a difference in the geometry of one or both of the turns in this constrained cyclic structure as compared to the turns in the open-ended hairpins. On the basis of NMR results,[32] one is type I′, the other type II′, but both are distorted from ideal ϕ,ψ values.

Spectral Simulation. To better understand the vibrational spectra obtained for these hairpin model peptides, the IR and VCD spectra of idealized β-turn and β-hairpin structures were simulated. All residues other than DPro and Gly were simulated as L-Ala for computational efficiency. This approximation has proven reliable for amide-focused vibrational analysis of peptides in a series of previous tests.[18,57,59,60] The turn segment alone

(57) Kubelka, J.; Keiderling, T. A. *J. Am. Chem. Soc.* **2001**, *123*, 12048.
(58) Hilario, J.; Kubelka, J.; Syud, F. A.; Gellman, S. H.; Keiderling, T. A. *Biopolymers* **2002**, *67*, 233.
(59) Bour, P.; Kubelka, J.; Keiderling, T. A. *Biopolymers* **2000**, *53*, 380.

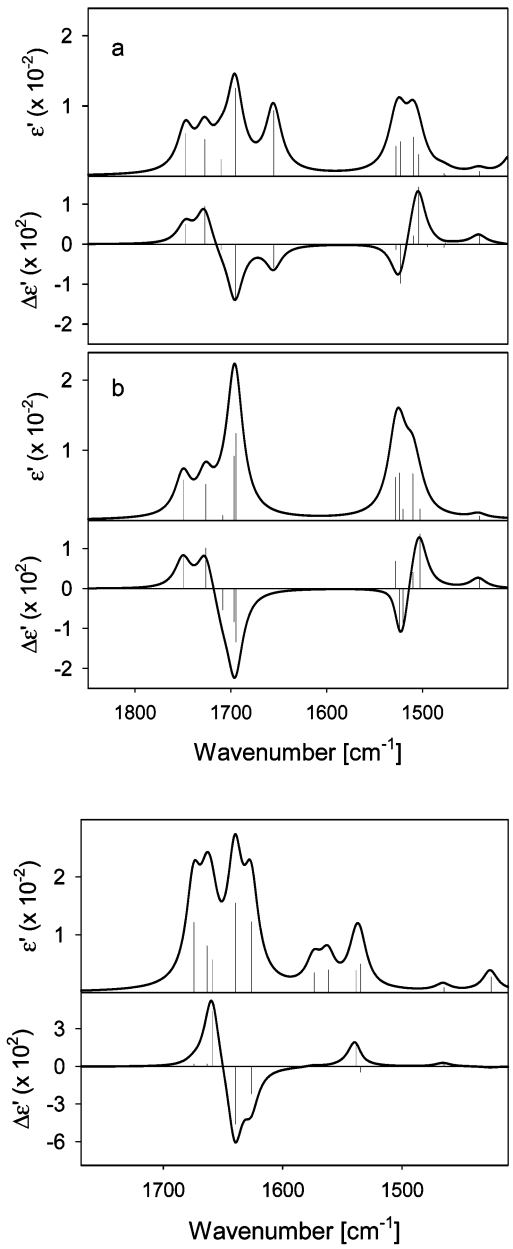

Figure 5. Ab initio simulated amide I and II IR and VCD spectra for type I′ β-turn models derived from the cyclic β-sheet peptide ^{D}PGcyc. (a) Ac-A^{D}PGA-NH-CH_3 (^{D}PG5), (b) Ac-A_2GA-NH-CH_3 (AG5), and (c) with 10 H-bonded H_2O molecules, ^{D}PG5·10H_2O. For (c) interfering H_2O vibrations were eliminated by transfer of the ^{D}PG5·10H_2O parameters onto the identical peptide without the solvent molecules. Intensity units ϵ' and $\Delta\epsilon'$ are the molar and differential molar extinction coefficients per amide group.

was simulated using an Ac-A^{D}PGA-$NHCH_3$ sequence; the approximate type I′ turn geometry being obtained from the NMR structure of ^{D}PGcyc.[47] The IR and VCD results for this sequence are shown in Figure 5a and there also compared to simulations obtained with an Ac-AAGA-$NHCH_3$ sequence (Figure 5b), with D-Pro replaced by L-Ala, to emulate the Asn-Gly-based turn.

Comparison of these two simulated IR spectra shows that the lowest-frequency amide I component of the turn spectrum is due to the C═O of the Ala-^{D}Pro amide linkage which in a β-turn is hydrogen bonded to the (i + 3) NH. Both the hydrogen bond and its tertiary amide nature (due to Pro) shift it to lower wavenumber.[55] The comparison Ac-AAGA-$NHCH_3$ calculation (no Pro) shows the equivalent mode in this sequence to be near degenerate with that of another H-bonded C═O. This characteristic low-frequency mode for the Ala-^{D}Pro linkage is indeed seen experimentally, compare spectra for ^{D}PG4 and NG4 in Figure 2. However, all calculated amide I frequencies are too high, since solvent effects were left out of our simulations;[61] thus, relative shifts of components are the basis for comparison. The C═O groups (^{D}Pro-Gly and Ala−Gly amides) directed "out" from the turn contribute to the amide I at relatively high frequencies due to their lacking H-bonds (the difference is overestimated here due to our calculating peptides in a vacuum). Similar calculations for turns with longer "tails," i.e. short hairpins, give consistent IR simulations.

The two (Ac-A^{D}PGA-$NHCH_3$ and Ac-AAGA-$NHCH_3$) computed VCD spectra are also very similar, with the highest-intensity IR band correlated to the highest-intensity (negative) VCD feature. The two "outer" amides of the turn (^{D}Pro-Gly and Gly-Ala) yield positive VCD in the simulation. This amide I shape is consistent with the negative couplet VCD found experimentally for just the turns (Figure 2), including the relative intensities of the negative components in each. The contributions of each amide C═O to these amide I normal modes are graphically illustrated in Figure 6. In the ^{D}P−G case, each mode has a dominant contribution from one residue, being remarkably localized, while for A−G there is a greater mixing of local modes. The overall computed amide II VCD is predicted to have a couplet shape, but since these peptides were measured in D_2O, there are no experimental amide II VCD. [Amide II′ modes occur at ∼1450 cm^{-1} and are overlapped by side chain and HOD absorbances.]

In an attempt to compensate theoretically for solvent effects, a similar calculation was carried out for solvated Ac-A^{D}PGA-$NHCH_3$ by incorporating 10 H_2O molecules explicitly hydrogen bonded to the peptide.[50] In this case, H-bonds to the solvent shift the amide I frequencies down to more realistic values (ranging from 1625 to 1675 cm^{-1}), distribute the dipole strength over the IR band, and reduce the separation between the turn and internally H-bonded modes (Figure 5c). However, the basic amide I VCD pattern is preserved, the feature originating predominantly from Ala-^{D}Pro is still lowest in frequency, and that from ^{D}Pro-Gly is highest. The computed solvated amide II VCD now effectively becomes a single positive band, which occurs at somewhat higher frequency than for the unsolvated turn. The amide I VCD pattern for this hydrated peptide more closely resembles that found (Figure 2) in our experimental results since the positive intensity coalesces to one mode, which is primarily a contribution of three local C═O vibrations.

If the ab initio turn and two-strand sheet calculations are combined, then spectra for the entire idealized hairpin sequence can be simulated by transfer of parameters. These results are in Figure 7, showing simulated spectra for the two-strand segment (in a vacuum) and its incorporation into the hairpin and cyclic models. The above spectral behavior for the turns is preserved in these larger structures. Now the intense negative VCD still correlates best with the intense IR peak, but the β-strand features are seen to overlap turn features. Nonetheless, for comparison with simulations for just the strands (Figure 7a), the high-frequency positive VCD features in the hairpins are best assigned

(60) Kubelka, J.; Keiderling, T. A. *J. Am. Chem. Soc.* **2002**, *124*, 5325.
(61) Kubelka, J.; Keiderling, T. A. *J. Phys. Chem. A* **2001**, *105*, 10922.

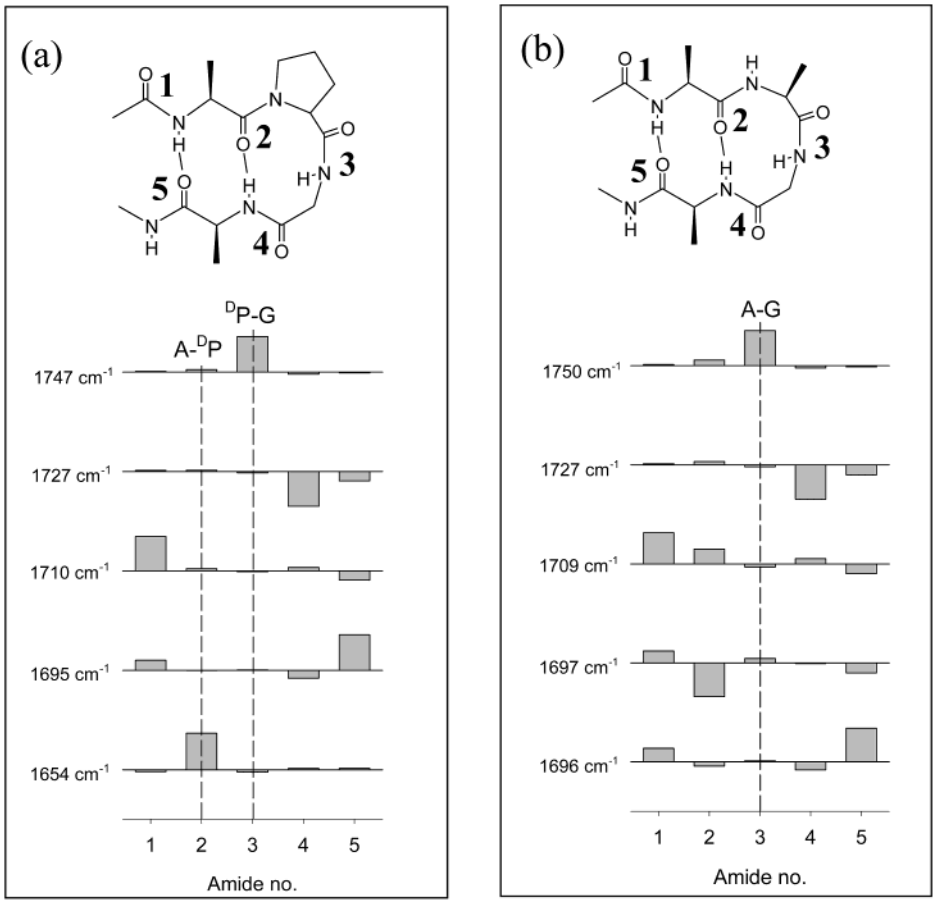

Figure 6. Amide I normal modes represented as amide C═O stretching amplitudes for type I′ β-turn models (a) [D]PG5, (b) AG5. Upward- and downward-pointing bars correspond to C═O bond stretching and contraction, respectively, and their length indicates the relative contribution. Numbering of the amide groups is indicated on schematic drawings of the model structures (top). [D]P-G and A-G are the $(i + 1)-(i + 2)$ amide linkages in the center of the turn, A-[D]P is the tertiary amide linking to the Pro residue.

to the turn, and the above computational results for the hydrated turn give us confidence that these features will persist in real solvated molecules. For the [D]Pro-based hairpins, the low-frequency amide I component is again associated with the tertiary amide C═O from the Ala-[D]Pro linkage which also provides the C═O in the hydrogen bond that completes the β-turn.

Mixed Solvent. To mimic the effect of residing in a hydrophobic pocket of a protein, we titrated each hairpin with varying amounts of 2,2,2-trifluoroethanol (TFE) at 20 °C. TFE promotes sheet or helix formation by reducing the water activity, the result depending on the structure propensity of the sequence. Results in Figure 8 for the Asn-Gly- and [D]Pro-Gly-based hairpins suggest TFE induces an increase in β-sheet structure as indicated by the increase in negative ellipticity at 215 nm and increase in positive ellipticity at 195 nm and the approach to a common band shape for all three. In all cases maximum conversion of these hairpins to greater β-sheet structure occurs at approximately 50% TFE (v/v). For NG12 and [D]PG12 further titration past 60% TFE (not shown) resulted in conversion to structures with spectra that are more difficult to evaluate but may have some helical character. This is evidenced by an intense positive ECD at 185 nm and negative at 203 nm with a shoulder at ∼220 nm (NG12) compared to a decrease in ellipticity at 195 nm and an increased and greatly broadened negative band at 218 nm ([D]PG12). [D]PG16 was not measured above 60% TFE. The lack of isodichroic points suggests that this solvent-induced transition samples multiple states. [D]PG12 undergoes a 50% increase in ellipticity at 215 nm, while NG12 changes by 62% and [D]PG16 shows the largest ellipticity change at 231%, which is probably not all due to sheet formation. Parallel FTIR experiments (not shown) have the main amide I′ band for both NG12 and [D]PG12 in 40% deuterated TFE (TFE-OD) shifting $\sim 5-6$ cm^{-1} to higher frequency which could correlate to a reduction of solvent hydrogen bonding to backbone carbonyls or reduced polarity of the surrounding medium (solvent).[61] The corresponding VCD spectra of these hairpins in TFE display only a single negative band instead of the couplet observed for the native states.

Thermal Denaturation. Thermal denaturation experiments were performed on selected hairpins using ECD and FTIR. Figure 9 (top row) shows the SVD reconstructed experimental ECD spectra, which removes some of the spectral noise component (using only the first four basis spectra), for the three hairpins over a 5−90 °C temperature range (arrows indicate direction of spectral intensity change with increase in temperature). Thermal-unfolding measurements performed on the cyclic peptide (not shown) resulted in only very small changes between low- and high-temperature spectra, which is consistent with its very stable structure, as expected. In all hairpin experiments, the largest ECD spectral change as a function of temperature occurred at wavelengths below 200 nm and around 230 nm,

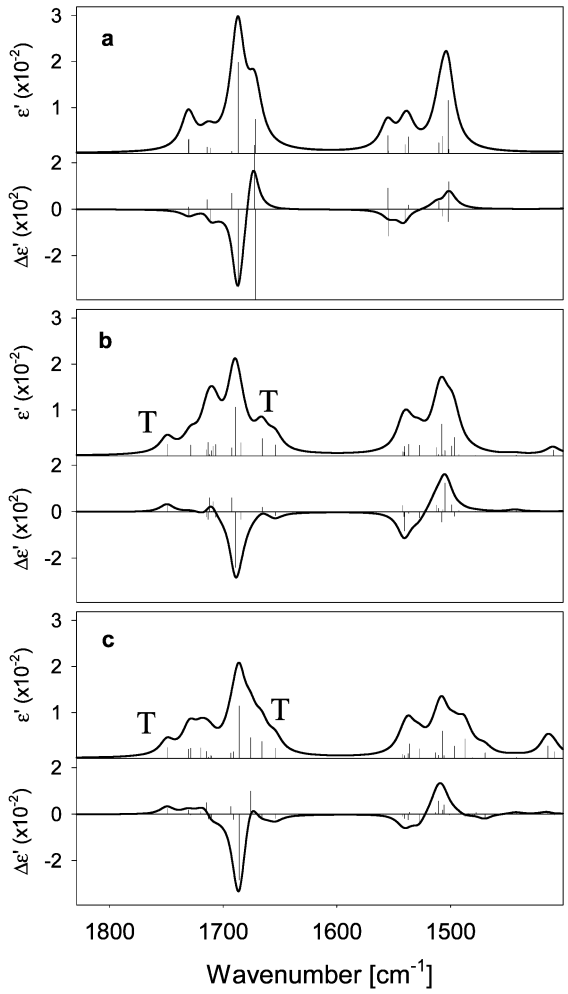

Figure 7. Simulated IR and VCD spectra for segments of the cyclic β-sheet peptide ^{D}PGcyc: (a) two-stranded β-sheet (Ac-A_3-NH-CH_3 strands), (b) the hairpin Ac-$A_5{}^{D}PGA_5$-NH-CH_3 with type I′ β-turn, and (c) the complete cyclic β-sheet peptide ^{D}PGcyc. The spectra were simulated by transfer of parameters from shorter fragments. "T" denotes contributions primarily originating in the turn residues.

the region of the far UV most impacted by aromatic residues. The change in the 230 nm region is consistent with a loss of structure for the hydrophobic core of the hairpin. However, ECD in the nominal β-sheet region at 215 nm is virtually invariant with temperature. The near isodichroic nature of these ECD suggests that the spectral responses are dominated by two conformations in each case. Below each set of spectra are shown the corresponding amplitude changes of the second SVD component as a function of temperature, which illustrate the very broad thermal transitions characteristic of these hairpins and confirm that a fully folded state is not achieved for any of these model hairpins. Thermal unfolding was also monitored by FTIR for just the ^{D}Pro-Gly-containing models, and the results proved to be consistent, with a linear increase in frequency with increasing temperature (^{D}PGcyc: 1634 → 1638, ^{D}PG12: 1638 → 1643, ^{D}PG16: 1640 → 1649, where frequencies are amide I′ maxima, data not shown).

Chemical Denaturation. Attempts to obtain equilibrium thermodynamic parameters for chemical unfolding of selected hairpin models proved unfavorable in that guanidine hydrochloride denaturation experiments yielded nonsigmoidal responses to added denaturant concentration. A comparison of ECD spectra for the native and denatured (high-temperature and high guanidine hydrochloride) forms of ^{D}PG12 is presented in Figure 10. While the GdnHCl denatured form loses a majority of its ellipticity above 200 nm, the thermally denatured form still retains a significant ECD band shape and intensity. This suggests that the final states of this hairpin model are substantially different under these two unfolding conditions. Similar results were obtained for NG12 and ^{D}PG16.

Discussion

Native Hairpin Spectral Characterization. Our results extend the understanding of the spectral properties of these model β-hairpin structures in aqueous solution and relate them to their structural properties that have been previously obtained primarily from NMR.[32] They offer further confirmation that short β-sheet hairpins can form in aqueous solution and that ^{D}Pro in the $i + 1$ position has a stereochemical advantage over proteinogenic, L-amino acids[34,62,63] for association of a β-turn with β-strands to yield a structure having a right-handed twist, as judged by the relative spectral band shapes of NG12 and ^{D}PG12 (Figure 4). Even short β-sheet hairpins (12 residues), if stabilized by a ^{D}Pro-Gly turn, have spectral characteristics replicating some aspects of the FTIR, ECD, and VCD band shapes found in larger, multiply stranded β-sheet-containing proteins. We find that increased sheet content in these hairpin models is accompanied by a frequency shift in the amide I′ IR to 1634 cm^{-1}, by an increase in ECD negative ellipticity at 215 nm, and an increase in positive ellipticity at 195 nm. These are all normally expected behaviors of β-sheet structures such as found in proteins without significant helix content and normally having relatively short, typically twisted strands. These observations on small hairpin models argue against comments found in the literature suggesting that hairpin spectra are somehow unique or that traditional spectral measurements do not distinguish β-sheet character.[64,65] However, these spectra do not replicate those of highly β-sheet homo- and heteropolymer polypeptides or denatured proteins which are generally characterized as aggregates and probably have extended, relatively flat sheets. Thus, if properly interpreted, optical spectra do indeed yield a useful structural analysis of these peptides. Nonetheless, it is important to use multiple techniques and to account for possible sources of interference such as aromatics or H-bonding to solvent as well as to account for the overlap of spectral components due to other structural elements for peptides of mixed conformation. As recently shown by Sreerama and Woody,[56] proteins that have substantial β-sheet content as well as significant PLP II (poly-L-proline-like extended left-handed twist) segments can have highly distorted ECD spectra that more resemble those of a random coil. Furthermore, such optical studies, while normally providing data related to the average contribution of all the structural components in the sample, can offer a different insight than that from the site-specific data available from NMR or crystallography.

(62) Awasthi, S. K.; Raghothama, S.; Balaram, P. *Biochem. Biophys. Res. Commun.* **1995**, *216*, 375.
(63) Haque, T. S.; Little, J. C.; Gellman, S. H. *J. Am. Chem. Soc.* **1996**, *118*, 6975.
(64) Arrondo, J. L. R.; Blanco, F. J.; Serrano, L.; Goni, F. M. *FEBS Lett* **1996**, *384*, 35.
(65) *Infrared Analysis of Peptides and Proteins: Principles and Applications*; Haris, P. I., Ram Singh, B., Eds.; ACS Symposium Series; American Chemical Society: Washington, DC, 2000; p 54.

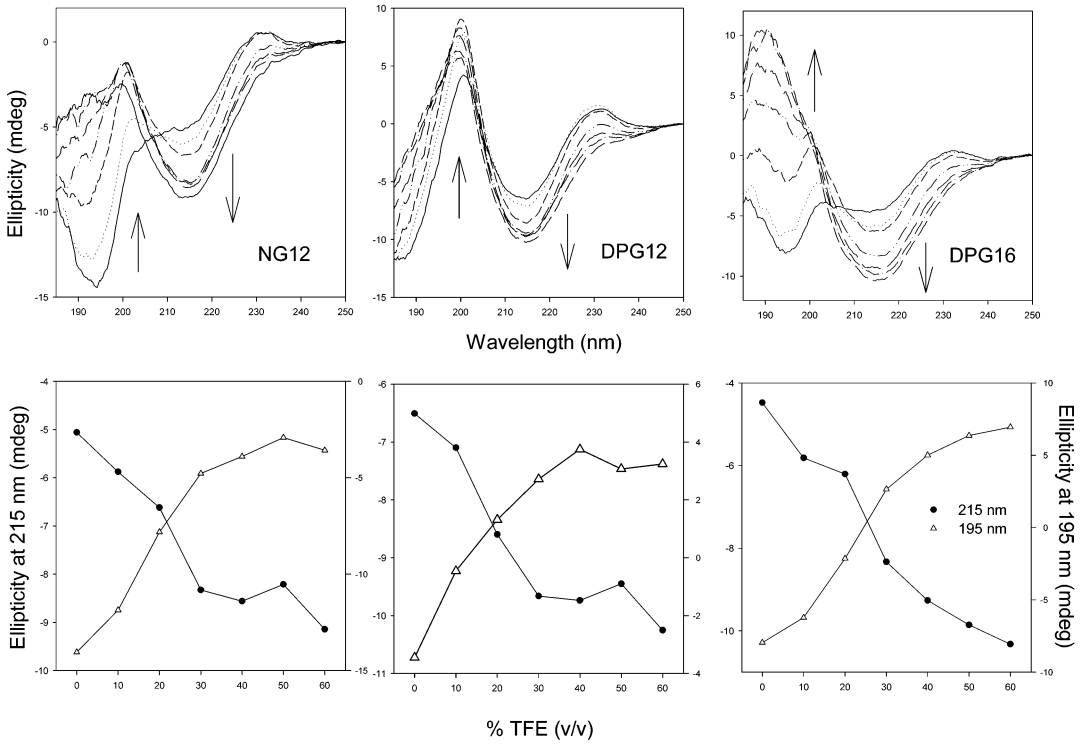

Figure 8. (Top row) Titration of selected β-hairpin models with TFE as monitored by ECD. Within each titration, the peptide concentration remained constant by dilution of stock peptide into appropriate %TFE solutions. (Bottom row) Ellipticity of the main positive (195 nm) and negative (215 nm) CD bands as a function of %TFE (v/v) indicate the initial TFE-induced change in the peptide has a plateau around 50% TFE. (Bottom row) As noted in the text, peptides in higher TFE concentrations produced spectra not easily interpretable as originating from β-structure.

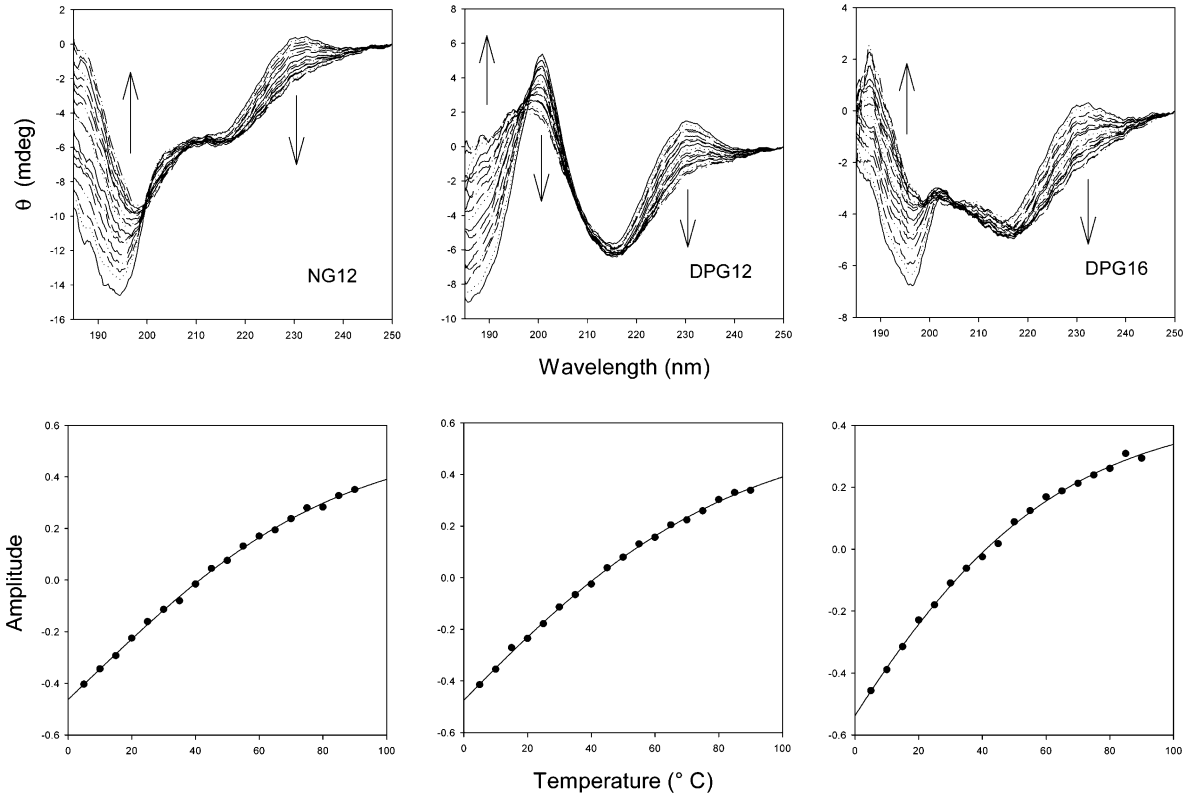

Figure 9. (Top row, spectra) ECD thermal denaturation spectra for selected β-hairpin models, NG12, ^{D}PG12, ^{D}PG16 (left to right). Spectra shown are SVD reconstructed spectra (to eliminate noise component). (Bottom row, amplitudes) Amplitudes of the second SVD component, which is a measure of the spectral variation as a function of condition showing very broad transitions.

The VCD spectra presented here are the first to be measured for β-sheet hairpins in water (a preliminary conference communication on two of these molecules has appeared[58]). Polavarapu and co-workers have reported a VCD study of similar

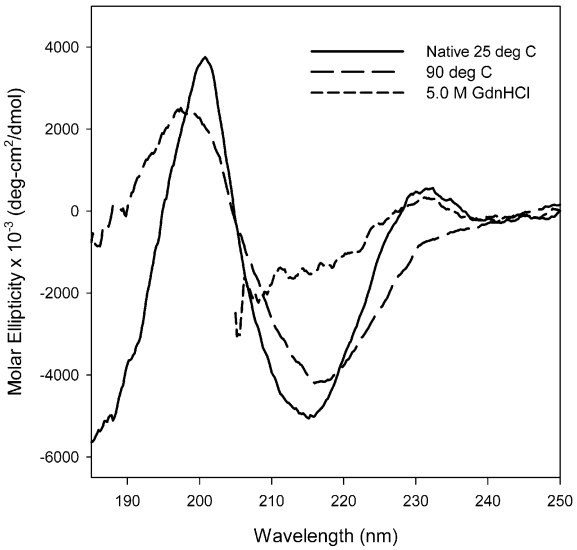

Figure 10. Comparison of the ECD of native (solid line), thermally denatured (dashed line), and GdnHCl denatured (dotted line) forms of ^{D}PG12, indicating a significant difference exists between the two denatured forms, with the thermally denatured form still possessing significant ECD intensity over the 230−210 nm region which may be indicative of remaining structure. These results indicate a different extent of unfolding under each condition (different end states).

^{D}Pro-Gly-stabilized hairpins in $CDCl_3$.[37] Their observed amide I′ VCD are dominated by couplet band shapes associated with the *local* left-handed helicity of successive carbonyls of each strand's peptide backbone. As noted above, two associated, antiparallel β-strands normally have an overall right-hand twist (since the sheet twist is determined by H-bonding of alternate C═O groups), but the sequential C═O helicity is left-handed. Due to this left-handed strand helicity,[5] the twisted β-sheet and β-strand VCD tend to resemble the PLP II VCD. The spectra obtained here for ^{D}Pro-Gly-based hairpins in aqueous solution (Figure 4) are in qualitative agreement with the patterns previously reported by Polavarapu and co-workers[37] for such peptides in a nonpolar organic solvent. Those also had an intense negative for the main amide I′ IR band and a positive for the higher-energy components. Simulation results (Figure 7) show that the higher-frequency (positive) features arise from the C═O groups on the turn residues (which are not internally H-bonded) and that the main (negative) peak has contributions of both sheet and turn, particularly from interstrand H-bonded amide C═O groups. The lowest-frequency mode is confirmed to be due to the Val-^{D}Pro amide (which forms the H-bond to close the turn) for the ^{D}PG*n* model hairpins.[55]

The ECD spectra all of the hairpin models, except the cyclic variant, contain evidence for a considerable amount of random coil type structure in addition to the turn formation. This is most likely attributable to end fraying effects of the hairpins. Since such random coil structures in peptides are often locally similar to a PLP II left-handed twist structure[52,53,66,67] and since such structures have distinct and strong ECD and VCD, difficulty in spectral analysis of β-sheet-to-coil transitions results.[56,67] Increase in the sheet content of these hairpins can be induced by addition of a cosolvent (TFE), which is sometimes used to mimic a more hydrophobic environment (i.e. such as the interior of a protein) and thereby increase the probability of forming cross-stranded intramolecular hydrogen bonds characteristic of the β-sheet structure. However, the end result is quite different for ^{D}PG12 and ^{D}PG16 (in the far UV), suggesting a real structural difference.

Results from IR band analysis show that 51%, 40%, and 33% of the integrated amide I′ intensity, for models ^{D}PG12, ^{D}PG16, and ^{D}PGcyc respectively, arises from the component at ~1634 cm^{-1} (this feature is often assigned as the major fraction of the amide I intensity for residues H-bonded in a β-conformation and its intensity is commonly used to determine fractional β-sheet content in proteins[65,69]). While this result may seem contrary to NMR results,[35] in fact, relative percentages here should correlate to the fraction of all amides that are found in a certain environment but may require rescaling to reflect quantitative β-sheet content. By using a very simple approach that assumes among other things that all C═O stretches contribute equally to the amide I dipole strength since the ^{D}PG12 model contains 11 total amides (including the tertiary amide, thus $0.51 \times 11 = 5.6$) an estimate of the number of amides in the β-conformation for the folded state is obtained. By contrast for ^{D}PG16, $0.40 \times 15 = 6.0$ gives a somewhat larger contribution in the longer hairpin. This simple analysis suggests that a similar number of amides comprise the stable β-hairpin core (H-bonded strands) in each, with the ^{D}PG16 model perhaps having slightly more (especially, if rescaled), as is also suggested by NMR.[35] To help evaluate the limitations of this approach, we can make reference to the cyclic peptide, ^{D}PGcyc, as a maximally folded hairpin as was done in the NMR analysis. The ^{D}PGcyc integrated IR intensity yields 0.33×14 amides = 4.6 amides, or less than 6, which would be the ideal number of H-bonded carbonyls in such a constrained structure (Figure 2). Thus, the apparently low values found for ^{D}PG12 and ^{D}PG16 cannot be interpreted in an absolute sense but should be viewed only relative to each other. The higher degree of fraying in the termini in ^{D}PG16 may contribute to its lower than expected value.

As an alternate test of the validity of this approach, we can also perform the same analysis for the percent area of the resolved amide I′ component arising from the Val-^{D}Pro tertiary amide. Of course, the ideal, simple analysis number should be 1 amide for this band, but for ^{D}PG12 and ^{D}PG16, we arrive at 2.3 and 1.5, respectively. This deviation suggests either some error in the deconvolution and band fitting or, more likely, substantial mixing occurring between the amide I′ modes of the chain and the H-bonded tertiary amide of the turn. The fact that this turn value is high while that for the β-strand residues (above) is low, is consistent with the sheet and turn modes being mixed and the intensity transferring from strand to turn-dominant mode. It is also consistent with our simulations which indicate (Figure 7) that the predominantly Ala-Pro amide I mode is more intense than the average of the other amide I modes, but this simulated variation is less than is seen experimentally for the ^{D}PG12 hairpin. Such effects have previously been found in isotope-labeled β-sheet studies, where, due to the ^{13}C substitution, amide I modes of labeled residues are shifted down in frequency and anomalously enhanced in intensity much as is

(66) Keiderling, T. A.; Xu, Q. *Adv. Protein Chem.* **2002**, *62*, 111.
(67) Shi, Z., Kallenbach, N. R., Woody, R. W. *Adv. Protein Chem.* **2002**, *62*, 163.
(68) Yasui, S. C.; Keiderling, T. A. *J. Am. Chem. Soc.* **1986**, *108*, 5576.
(69) Keiderling, T. A. In *Circular Dichroism: Principles and Applications*, 2nd ed.; Nakanishi, K., Berova, N., Woody, R. A., Eds.; Wiley: New York, 2000; p 621.

seen for the Val-^{D}Pro amide.[57] Due to such mixing, IR intensity-based determinations of secondary structure distributions can only be viewed as qualitative and must remain complementary to evaluation of other spectral parameters in terms of structure.

An examination of the ^{D}PGcyc (containing 2 Val-^{D}Pro tertiary amides) IR spectra (Figure 5) reveals a large contribution from the low-frequency mode evident at 1613 cm^{-1}. On the basis of band fitting, this intensity would suggest 4.6 amides contributing to the mode at 1613 cm^{-1}, which ideally it would be only 2, which is remarkably consistent with the ^{D}PG12 result above (2.3 instead of 1). These cyclic peptide intensity results, high for the turn and low for the strand, confirm that there is considerable mixing between the modes of different conformational types. The fact that the DPG16 value is smaller, not fitting this pattern, suggests that the contribution from the additional frayed residues impacts this simple analysis. Finally, the fact that the ECD band shape of ^{D}PG16 has such a strong random coil component substantiates the IR analysis and is consistent with its VCD having more intensity than ^{D}PG12, since the sheet component VCD will be very weak and the coil VCD stronger.[57,68,69] Given the even stronger mixing that would occur between electronic transitions,[38,67] attempts to deconvolve the ECD into independent turn and strand contributions would fare even less well than did our efforts above with the relatively localized IR transitions.

The overlap and mixing between the characteristic turn and sheet vibrations is also evident from theoretical simulations of the vibrational spectra. The low-frequency amide I component of the sheet segment (Figure 8a) and its associated positive VCD overlaps the tertiary amide turn region. Similarly, the high-frequency sheet vibrations approach the high-frequency vibrations of the turn X-Gly (X = Ala or ^{D}Pro) linkage. The larger and more stable the β-sheet is, the larger is the expected splitting between low- and high-frequency amide I components.[57] As a consequence, the sheet vibrations may change in overlap with the turns as the sheet content varies. This is consistent with the amide I deconvolution results for the cyclic model, ^{D}PGcyc, which is presumed to have the most stable and well-formed two-stranded sheet segment. Furthermore, the comparison between isolated and solvated turn simulations suggests that hydrogen bonding to solvent may contribute to delocalization of the turn amide I vibrations, resulting in shifting of characteristic low- and high-frequency turn modes closer together (Figure 5c as compared to Figure 5a, b). Therefore, more mixing of the turn and sheet amide vibrations can be expected in solution. Finally, in our simulations of β-sheet spectra,[57,70] it was clear that dipole intensity was transferred to the lowest-frequency, alternate phase mode for β-sheet structures, and these in turn can couple to the turn modes.

The results from optical spectra do not contradict what is observed in NMR,[35] due to the fact that different techniques detect contributions to the structure with varying sensitivity. The β-strand populations have been determined by α-proton and α-carbon chemical shifts which are sensitive to secondary structure, but to other environmental factors as well. While stabilization of the β-hairpin population was found upon strand lengthening with both NMR[35] and IR (above), our results suggest that lengthening the hairpin model with Thr, which is not very hydrophobic although it has high β-sheet propensity,[71] leads to more disordered tails. The β-hairpin core of both ^{D}PG12 and ^{D}PG16 would have similar sheet contents based on our IR analysis, while NMR results show ^{D}PG16 with higher β-population.[35]

Hairpin Unfolding. Denaturation experiments for these small peptide models show very broad thermal unfolding transitions with no apparent sigmoidal character. Even at the lowest temperature studied, ~5 °C, an initially stable folded state is not achieved, since the spectra immediately start to change upon incremental temperature increase, most clearly seen by the initial linear change of the SVD amplitudes. These changes continue, indicating unfolding of the hairpins to whatever extent is viable upon thermal perturbation. Since in all sets of temperature spectra there is an apparent isodichroic point at ~200 nm and because all models are completely reversible under thermal denatuation, it is still *possible* to conclude that these small β hairpins melt in a two-state manner. Consistent with the broad ECD transitions, results from FTIR showed a nearly linear change in frequency as a function of temperature, with no detectable sigmoidal character. Our data suggest that the folding/unfolding of β-sheet strands, in the absence of tertiary structure interactions, occurs with little or no free-energy barrier between native and unfolded states, leading to broad thermal transitions. This implies that forming the turn initiates structure formation and that the strands come together as temperature is decreased. In fact, our DPG4 results suggest that this ^{D}Pro-Gly-based turn might be so stable as to effectively not unfold (locally). Other reports of cooperative transitions in hairpins based on the 16-residue G-peptide where all but the terminal residues have a common melting transition temperature, T_m, (NMR-based[72]) might seem in contrast to this behavior, yet those transitions are just as broad as observed in our models. More recent NMR studies of a set of β-hairpin models, to the contrary, have interpreted their broad transitions and variations in T_m as evidence for a multistep model for β-hairpin folding, although these transitions are also very broad.[73] Previous studies of the variation of ^{D}PG12 chemical shifts have been interpreted as indicating the populations of β-residues were correlated.[32,75] The variance between detailed thermal variation behavior and structural interpretations suggests that definitions of cooperative transition and two-state behavior need refinement for these systems.

Noncooperative unfolding transitions have been found for selected three-strand β-sheet systems containing the same ^{D}Pro-Gly turns as used in this study, as monitored by FRET, FTIR, and ECD.[24] However, other workers have shown that if the stability of the folded state is significantly increased over the denatured state, e.g. through greater stabilization of β-strand association (such as incorporating Trp-Trp or other hydrophobic cross-strand pairings), then sharper spectral transitions providing evidence of structural change and conventional cooperativity can be conferred onto even a hairpin system.[16,17,74,75] This stability can also be observed in the designed 20-residue miniprotein, Trp cage, where interaction occurs between Trp and Pro, which displays characteristic two-state unfolding.[28] By contrast, results of thermal denaturation as monitored by intrinsic

(70) Kubelka, J.; Keiderling, T. A. *J. Am. Chem. Soc.* **2001**, *123*, 6142.
(71) Minor, D. L.; Kim, P. S. *Nature* **1994**, *371*, 264.
(72) Jas, G. S.; Eaton, W. A.; Hofrichter, J. *J. Phys. Chem. B* **2001**, *105*, 261.
(73) Santiveri, C. M.; Santoro, J.; Rico, M.; Jimenez, M. A. *J. Am. Chem. Soc.* **2002**, *124*, 14903.
(74) Espinosa, J. F.; Gellman, S. H. *Angew. Chem., Int. Ed.* **2000**, *39*, 2330.
(75) Espinosa, J. F.; Syud, F. A.; Gellman, S. H. *Protein Sci.* **2002**, *11*, 1492.

tyrosine fluorescence (not shown) revealed that the fluorescence intensity changes with temperature for the peptide models studied here were similar to those of free tyrosinamide. This suggests that the lone tyrosine residue is not hydrophobically protected and thus does not provide a useful probe of structural change for these hairpins.

Mixed Solvent Studies. Measurements in TFE were performed to examine the ability of the hairpin models to attain a more developed β-sheet structure and to examine the effect of a more hydrophobic environment in enhancing hairpin stability. We cannot determine a sheet population from this TFE titration experiment due to the uncertainty in determining the ellipticity of the fully folded and unfolded state and the inability to ascertain if the final state is actually a hairpin (at very high TFE concentrations greater than 60%, ECD spectra become broader and more intense and less identifiable as β-sheet type spectra). These results do suggest an ordering of initial (aqueous) native structure in terms of overall fraction of β sheet as ^{D}PG12 > NG12 > ^{D}PG16 based upon the relative ellipticity change. This suggests that ^{D}PG12 has the highest fraction of residues in a β-sheet structure, while the longer ^{D}PG16 has the least by assuming that the extent of ellipticity change is related to the degree of folding necessary to attain a β-sheetlike state. However, if the ends of the ^{D}PG16 hairpin strands form PLP II-like random coil segments, the ECD will probably not be a reliable indicator.[56]

GdnHCl unfolding experiments additionally provided evidence for unfolding transitions that were not cooperative, which further supports the existence of little free-energy barrier between the native and unfolded states. Near-UV ECD spectra of ^{D}PG16 and free tyrosinamide resulted in identical spectral responses under native and GdnHCl conditions, providing added confirmation of the tyrosine being solvent-exposed in these hairpin models. However, an interesting comparison results from the spectra of the final states obtained with the temperature and the chemical denaturation experiments (Figure 10). These suggest that considerable structure is retained in the temperature-denatured "end-state" as compared to the GdnHCl denatured "end state".

Conclusions

Despite the instability of these selected hairpin models under environmental perturbation, spectroscopic results confirm that β hairpins can form autonomously in water. Even though these hairpins do not fold to a 100% population, their degree of folding (particularly for ^{D}PG12) indicates that β hairpins (these being without strong aromatic interactions) can possibly serve as nucleation sites for β-sheet proteins. Clearly, if the right residues are present and when they are enhanced by tertiary interactions, the hairpin motif can be stabilized. Finally, these results demonstrate that conventional β-sheet response can be detected in both ECD and FTIR with well-formed, isolated β-hairpin structures.

Acknowledgment. This work was supported in part by a grant from the donors of the Petroleum Research Fund administered by the American Chemical Society, and the ECD spectrometer was obtained through an NSF Grant (CHE-00-91994). We wish to particularly thank Professor Sam H. Gellman for suggesting that we study the ^{D}Pro-Gly system and for providing some initial samples prepared by Dr. Faisal A. Syud, Professor Robert W. Woody for sharing his manuscript on β-sheet ECD before publication, and Professor Max Diem for pointing out the tertiary amide effect on Pro amide I frequencies.

JA030039E